Coupled Mutagenesis Screens and Genetic Mapping in Zebrafish

John F. Rawls,[1] Matthew R. Frieda, Anthony R. McAdow, Jason P. Gross, Chad M. Clayton, Candy K. Heyen and Stephen L. Johnson[2]

Department of Genetics, Washington University School of Medicine, Saint Louis, Missouri 63110

Manuscript received October 18, 2002
Accepted for publication November 26, 2002

ABSTRACT

Forward genetic analysis is one of the principal advantages of the zebrafish model system. However, managing zebrafish mutant lines derived from mutagenesis screens and mapping the corresponding mutations and integrating them into the larger collection of mutations remain arduous tasks. To simplify and focus these endeavors, we developed an approach that facilitates the rapid mapping of new zebrafish mutations as they are generated through mutagenesis screens. We selected a minimal panel of 149 simple sequence length polymorphism markers for a first-pass genome scan in crosses involving C32 and SJD inbred lines. We also conducted a small chemical mutagenesis screen that identified several new mutations affecting zebrafish embryonic melanocyte development. Using our first-pass marker panel in bulked-segregant analysis, we were able to identify the genetic map positions of these mutations as they were isolated in our screen. Rapid mapping of the mutations facilitated stock management, helped direct allelism tests, and should accelerate identification of the affected genes. These results demonstrate the efficacy of coupling mutagenesis screens with genetic mapping.

GENETIC screens provide an invaluable tool in the identification of genes required for specific cellular and developmental processes. In animals, this approach has been most successful in the *Caenorhabditus elegans* and *Drosophila melanogaster* model systems, where large-scale genetic screens have revealed mechanisms underlying many aspects of animal development and physiology. In contrast, forward genetic analysis of biological processes in vertebrates has traditionally been an exceptionally strenuous task. This problem has been addressed recently through the successful use of zebrafish (*Danio rerio*) in a growing number of genetic screens (Driever *et al.* 1996; Haffter *et al.* 1996a; Henion *et al.* 1996; for review, see Patton and Zon 2001). These screens have resulted in an impressive collection of mutants defective for a variety of cellular and developmental processes, and the identification of genes affected in these mutants is providing new insights into vertebrate biology. Additionally, the pursuit of saturation mutagenesis and the creation of new techniques to assay biological processes are now compelling new generations of zebrafish mutant screens (Jagadeeswaran *et al.* 2000; Farber *et al.* 2001; Patton and Zon 2001).

This wealth of mutations is accompanied by the challenges of mutant stock management and identification of affected genes. These tasks are greatly facilitated by identifying the map position of individual mutations. Mapping of new mutations facilitates stock management through genotyping of heterozygous carriers, candidate gene identification, and testing for allelism to previously identified mutant loci. Therefore, the development of techniques that accelerate the mapping process should have widespread benefits for zebrafish genetics.

The need for more rapid mapping techniques is exemplified in the field of zebrafish pigment pattern biology for two principal reasons. First, the salient nature of pigment pattern phenotypes has resulted in the identification of several hundred zebrafish pigment pattern mutations (Johnson *et al.* 1995b; Haffter *et al.* 1996b; Henion *et al.* 1996; Kelsh *et al.* 1996; Odenthal *et al.* 1996; Rawls and Johnson 2001; this work). Second, our incomplete understanding of zebrafish pigment pattern biology compels further genetic analysis. Among the multiple cell types that comprise the zebrafish pigment pattern, the melanocyte (also called melanophore in poikilotherms) is the only pigment cell type common to both fish and mammals. Similar to other vertebrates, the melanocytes that comprise the zebrafish pigment pattern are derived from the neural crest, and the melanocytes of the pigmented retinal epithelium (PRE) are derived from the optic cup. Like other neural crest derivatives, melanocytes must be properly specified from neural crest progenitor cells, migrate to appropriate positions in the body to compose the pigment pattern, and persist through subsequent stages of development. Melanocytes therefore provide a good model for the analysis of cell fate specification, migration, survival, and organogenesis (for review, see Rawls *et al.*

[1]*Present address:* Department of Molecular Biology and Pharmacology, Washington University School of Medicine, 660 So. Euclid Ave., St. Louis, MO 63110.

[2]*Corresponding author:* Campus Box 8232, 4566 Scott Ave., St. Louis, MO 63110. E-mail: sjohnson@genetics.wustl.edu

2001). Furthermore, an understanding of melanocyte development in zebrafish may also provide insights into human melanocyte disorders such as vitiligo, Waarderburg syndrome, and melanoma. As our understanding of the mechanisms underlying zebrafish pigment pattern biology remains incomplete, new genetic screens are needed. The efficiency of new screens and the subsequent analysis of mutants will be greatly increased if researchers can rapidly map the resulting mutations.

Inbred lines provide a valuable tool in the mapping of mutant loci. Good mapping strains require extensive polymorphism between lines and reproducible alleles (*e.g.*, PCR product sizes) within lines. The inbred lines C32 and SJD generally meet these criteria. Each of these lines is >93% homozygous for simple sequence length polymorphism (SSLP) markers (Nechiporuk *et al.* 1999; S. L. Johnson, unpublished results), and more polymorphisms are evident between these lines than between either of them and WIK, another commonly used mapping strain (Nechiporuk *et al.* 1999). Furthermore, we find extensive single nucleotide polymorphisms (SNPs) between C32 and SJD lines. Initial analysis of expressed sequence tags (ESTs) and cDNAs suggests ~1 SNP every 100 bp in noncoding DNA and ~1 SNP every 300 bp in coding sequence between C32 and SJD (J. F. Rawls and A. R. McAdow, unpublished results). These SNPs will further facilitate the rapid mapping and refinement of meiotic maps in pursuit of positional cloning projects.

In mouse, the availability of SSLP markers that distinguish between haplotypes of different inbred strains has facilitated the management of F_3 mutagenesis screens and initial mapping of mutations derived from them (Kasarskis *et al.* 1998; Herron *et al.* 2002). Here, we describe a zebrafish mutagenesis screen that similarly incorporates inbred lines and genomewide mapping using SSLP markers. We improve upon the approaches of Kasarskis *et al.* (1998) and Herron *et al.* (2002) by performing our initial genetic mapping in the same F_2 haploid embryos in which the mutant phenotype is first observed. This is made possible by the relatively large clutch sizes usually obtained from zebrafish. Thus, by coupling the initial phenotypic screening with genetic mapping, we avoid the need to perform additional crosses for the initial mapping of the mutation, thereby substantially accelerating the mapping process and facilitating mutagenesis screen management.

Several methods exist for initial mapping of zebrafish mutations (Postlethwait *et al.* 1994; Johnson *et al.* 1995a; Singer *et al.* 2002), and in this study we describe a method to improve upon one of them. We first describe a panel of SSLP markers polymorphic between SJD and C32 at ~20-cM intervals throughout the zebrafish genome. We conducted a small-scale F_2 haploid screen for new mutants defective for embryonic melanocyte development (Walker 1999) and then used the marker panel in a bulked-segregant genome scan using DNA from F_2 haploid individuals to rapidly identify the candidate map positions of these new mutants (Michelmore *et al.* 1991). These candidate map positions were then confirmed by recombination analyses on individual haploids. Further, the identification of SSLP markers closely linked to mutant loci (on SJD haplotypes) provided surrogate markers for identification of carriers following introgression and stock management in the C32 background. The map positions indicated by this work also allowed us to test for and identify allelism between several of our new mutations and known loci. We show that by using the C32 and SJD inbred lines and this panel of polymorphic markers, new zebrafish mutations can be rapidly and accurately mapped as they are generated through mutagenesis screens. The incorporation of this technique into future zebrafish mutagenesis screens should accelerate the rate of initial mutant mapping, simplify stock management, and help focus subsequent investigations.

MATERIALS AND METHODS

Inbred lines: The original SJD inbred line was derived from a natural population collected in 1989, passed through two generations of full sibling matings, through two sequential generations of early pressure parthenogenesis (Johnson *et al.* 1995a), and finally through seven additional generations of full sibling matings, resulting in >98% homozygosity across the female meiotic map (see http://zfish.wustl.edu). Because original SJD stocks in our colony are predominantly male, we are currently introgressing genes from the C32 genetic background that dominantly promote female development into the SJD genetic background. We are carrying this introgression through eight sequential generations of backcross to the original SJD strain. We have several parallel lines that produce 25–50% females at the fifth or sixth backcross generation, breed well by natural crosses, and also easily yield eggs and sperm following squeezing for *in vitro* fertilization. We can currently provide fish from our SJD female introgression lines (six generations of sequential backcross, estimated <5% C32). A similar introgression of genes from SJD has been performed to enhance vigor in C32 stocks, and we can provide fish from our ninth sequential backcross generation (requests to S. Johnson).

Mutant screening: Adult SJD male zebrafish were mutagenized with *N*-ethyl-*N*-nitrosourea (ENU) according to Solnica-Krezel *et al.* (1994). Mutagenized SJD males (≥10) were bred with C32 females, and the resulting F_1 progeny were reared at 28.5°. F_1 stocks derived from different mutagenized males were sometimes mixed together, and thus we cannot always rule out the possibility that multiple isolates at the same loci are not the same allele. Clutches of eggs from individual F_1 females were collected, and each clutch was split in half. Half of each clutch was fertilized with sperm of the C32 haplotype to produce F_2 outcross lines, and half of the clutch was fertilized with UV-inactivated sperm to produce F_2 haploid embryos for phenotypic screening (Streisinger *et al.* 1981; see Figure 1). When >20 haploid embryos were available in a clutch, we split them between a group allowed to develop at 25° and a second group allowed to develop at 33° (505/604 clutches tested by these means).

Using a dissecting light microscope, we evaluated F_2 haploid embryos at multiple time points between 1 and 4 days postfer-

tilization (dpf) for defects in melanocyte development using wild-type haploid siblings as controls. We considered an F_1 founder successfully screened if at least eight F_2 haploid embryos were produced and evaluated. Haploid clutches displaying defects in melanocyte development in ~50% of individuals were identified, and the corresponding clutch of F_2 outcross fish was maintained. All staging of zebrafish embryos was performed according to Kimmel *et al.* (1995). Morphological descriptions of mutant phenotypes in the text are for embryos reared at 25°, except where noted.

Bulked-segregant PCR: Genomic DNA was isolated from individual mutant haploid embryos and their wild-type haploid siblings into 100 μl TE using standard protocols. Equivalent aliquots from individual embryo DNA preparations were pooled (7–14 individuals per pool) and then diluted 30-fold to generate mutant and wild-type DNA pools for each mutation. Three microliters from each diluted DNA pool was then used as template in 25-μl PCR reactions using primer concentrations of 1 μM. The reactions were amplified using the following protocol: initial denaturation at 92° for 3 min, followed by 36 cycles of 92° for 30 sec, 94° for 5 sec, 55° for 30 sec, and 72° for 90 sec, with a postamplification extension at 72° for 4 min. The resulting amplicons were resolved on 2% agarose gels and visualized with ethidium bromide. Error estimates are reported as standard deviation.

Nomenclature: We follow the general rules of zebrafish nomenclature for designating locus and allele names. Thus, locus names and abbreviations are registered with ZFIN, and each allele is assigned a unique allele name. Locus names are provisional, because they may correspond to previously identified but still unmapped mutations. Allele designations in this screen begin with *j* (for Johnson lab), followed by a number to indicate our locus designation (for instance, 1 represents *kit* and 121 represents *chloe*), a letter to indicate mutagenesis method (for instance, *e* represents ENU), and a final number to indicate order of isolation in our allelic series. Reported map positions refer to the MOP panel (Johnson *et al.* 1996; see Meiotic Maps at http://zfish.wustl.edu).

RESULTS

Identification of first-pass SSLP markers for bulked-segregant analysis: To identify SSLP markers for our first-pass panel for bulked-segregant analysis, we took advantage of the ~2000 previously published SSLP markers (Shimoda *et al.* 1999), as well as markers not yet published but available on the Massachusetts General Hospital website (http://zebrafish.mgh.harvard.edu). We first tested the first-pass markers suggested at the above web site, as appropriate. Additionally, we developed 40 SSLP markers derived from repeats identified in our EST project (Clark *et al.* 2001; see Table 1), which we mapped on the LN54 radiation hybrid panel (Hukriede *et al.* 2001), the MOP haploid panel (Johnson *et al.* 1996), and the HS meiotic panel (not shown; Kelly *et al.* 2000). We screened for markers that were ~20 cM apart, gave reliable amplification from C32 and SJD DNA, had significant size polymorphism between the C32 and SJD lines (generally >10 bp), and amplified both alleles in heterozygotes (to facilitate bulked-segregant analysis). We screened >500 SSLP markers for meeting the above criteria and selected a minimal panel of 149 markers spaced on average 22 ± 8 cM apart on the female meiotic map or 5 ± 7 cM from the apparent ends of the meiotic linkage groups. In a few cases, we had to accept markers >30 cM apart (intervals 39–77 cM on LG3, 55–95 cM on LG4, 0–32 cM on LG6, 98–141 cM on LG7, 75–112 cM on LG8, 2–43 cM on LG9, 37–68 cM on LG12, 5–39 cM and 55–87 cM on LG14, 6–44 cM on LG20, and 57–100 cM on LG 22). In these intervals, few SSLP markers were available, indicating that these regions have exaggerated rates of meiotic recombination. This suggests that these are relatively small physical regions, a notion that is generally supported by the low number of ESTs mapped to these regions (Hukriede *et al.* 1999; S. L. Johnson, unpublished results). Our preferred SSLP markers for first-pass screening by bulked-segregant analysis are listed in Table 2 and are also posted at http://zfish.wustl.edu.

Production and mapping of new melanocyte mutants: We performed a genetic screen for mutations that affect the development of the embryonic melanocyte pigment pattern (Figure 1). While melanocytes are not directly required for survival, genes required for melanocyte development may also be required for development of other essential neural crest derivatives (see Rawls *et al.* 2001). To facilitate the identification of melanocyte mutations that are lethal due to defects in neural crest stem cells or other essential neural-crest-derived cell types, we focused our screen on the phenotype of the embryonic melanocyte pattern. Since wild-type haploid zebrafish embryos are viable through 4 dpf and develop a relatively normal melanocyte pattern (Walker 1999), we screened for abnormal melanocyte phenotypes in haploid embryos (see materials and methods).

We screened F_2 haploid clutches representing 604 mutagenized haploid genomes and found 31 possible melanocyte mutants. Additionally, we added to our analysis two melanocyte mutants (*j108e1* and *j121e1*) identified in a previous early pressure parthenogenesis screen conducted in our lab. Of these mutants, we attempted to map 20 and were able to identify map positions for 19 (95%). Although 2 of our mapped mutants were subsequently lost (*j120e1* and *j130e1*), all others are currently maintained in our lab as breeding stocks or frozen sperm.

Mapping of new mutations was accomplished using bulked-segregant analysis (Michelmore *et al.* 1991; see Figure 1). Using selected polymorphic marker primers (Table 2), bulked-segregant PCR was performed on mutant and wild-type DNA pools from each mutant clutch (see materials and methods). Candidate-linked markers were identified as those in which preferential amplification of the SJD and C32 haplotypes was observed in the mutant and wild-type pools, respectively. Markers that suggested linkage in bulked-segregant PCR were then tested on DNA from the individual mutant and wild-type embryos that comprised the respective DNA pools. If linkage of candidate markers was confirmed on DNA from individual haploid embryos, then markers

TABLE 1

SSLP markers generated from zebrafish ESTs

Marker name	Primers	Repeat class	Allele size (bp) C32, SJD	Map position
fc27h08.x(wz7307.1)	ACGAACGAACAAACGAACG/ CCTTATTTCTTTTTCTGTTTTTGC	AAAG	290, 155	1:24
fb98a11.y(wz11681.1)	CAATTCTGCAATGACTTTCACA/ GTTCAGCGCTGTGCTCTCTA	CA	80, 90	1:99
fi03f10.x(wz3638.2)	CTGAGCCATTTCGTGTGTGT/ TAAAAAGAGGGAACGCTTGC	CA	145, 90	1:99
fb55d12.y(wz4079.2)	GGAACCCAAACCAGAGTGAA/ TAAAGGACGTCGTGGTCCAG	CA	80, 100	3:0
fc79b03.x(wz9400.1)	TGTGTTTTACGCGTGTTGTATG/ TTGTTGAAGAAGCGAGAGAAGA	GA	90, 80	3:33
fc63g04.y(wz12941.1)	CAAACTTTATCTTGGATGCGATT/ TTGAAATTTCTCAGTTTCTCTGGA	TA	135, 140	3:62
fc54e07.y(wz12784.1)	CCGTCTGTCTGTCTCTGCTG/ GCTACCAGCACCCTAAAGGA	ATG	225, 230	4:0
fc13d05.y(wz4816.2)	TGAAAGTGGAATGCTGGAAA/ TGAACCATCATCTCCAACGA	ATG	155, 145	5:103
fc22g02.x(wz12144.1)	CACTGTGTCGACCCCAGATT/ CGCCCTCTGCTGGTAAGTAA	AATG	160, 150	5:103
fi04e09.x(wz2877.1)	CAGCCCAAATTTTCCTTAGC/ TGTGTGTGTGCAGTGCAATTA	GA	130, 140	5:103
fc33b05.x(wz9906.1)	CAGAAGGCAAACCTCGAGTC/ TAGGGCAGATGAGCTGTGTG	AAAC	145, 135	7: 57
fd07h09.y(wz4810.1)	TCATGAAAACGGGACAAAGA/ TCATGAAGGTTTCTGTCTGACATT	GA	135, 125	7:77
fj30f10.x(wz9540.1)	TCGCATAATCATCGTTGTCA/ TTAAGTAACACATTCCACCCCTA	CA	115, 185	7:162
fi59h04.y(wz15291.1)	GCGTCCGAATAATATTACGTGTG/ TTGCCAGATATTGTGCAACG	AAT	180, 155	8:56
fk30a11.x(wz5446.1)	CAGGAGAGCCAATAGTTTAGCC/ TCCTAGATAAGCAGGATTTGCAG	AAAT	145, 190	8:72
fj86d02.y(wz6996.2)	CATGGCCAGCCGGATAAT/ GGAAAGCCGTGTAAAAGCTG	CA	155, 100	8:112
fe06c05.x(wz901.1)	AAAACACATGCCCAGACTGA/ TCGAGTGTAGGAGGAGCTTCA	CA	170, 80	8:112
fd14c10.y(wz9195.1)	TTCCTTGAAACTAGTAGATGGTTGG/ ACATGCACCAAGGGCTAAAA	AAC	235, 220	11:52
fd47h11.x(wz2225.1)	AGCCTGGCTTTAAAGGAACA/ CAACTTAACTCAAGTGAGCCCTTT	AAT	115, 105	11:58
fa99f08.x(wz6762.1)	ATGACCAAAATTGGTGCCTA/ GGGCTGCCAAACTTATAGGA	AATC	160, 150	12:68
fc41b11.y(wz5433.1)	GTGACTGCCCTTCCAGCTTA/ GGTTTCCCCCACAGTCTTAAA	ACTC	160, 150	12:80
fj22f07.x(wz5397.1)	TTCCCGTCTCCTGTTTGTTC/ TCATCACTCCCGATAACTGC	CA	145, 90	13:6
fj03e12.y(wz15601.1)	AAGCTGTGCAGTGGTCAAGA/ GCTGAGGTAGACACTCACACAGA	CA	110, 90	13:110
fj36c01.x(wz887.1)	ACGAGGACAGGGAGAGTGAG/ TGAGCCCCTGACTTTAATGC	GA	90, 80	14:69
fj01d05.y(wz37.1)	CCACAACGAAATCCACTGAA/ TGTTTGACTTTTCTGTCTTTCCA	CA	130, 100	14:118
fb62g12.y(wz5200.2)	CACGGCTTCTCTCAGAGCATA/ CAAAGTGCATATGAGTGTACTACGG	CA	130, 134	15:0
fi29b07.x(wz4996.2)	GGTCACCCTGGTGCACATA/ TGTGCCCACTCGAGTAAATG	CA	140, 125	15:0
fi34g12.x(wz5122.1)	AGTTCACGTCCGCTCAGATT/ CCCCGTCAAAAATGAACACT	CA	90, 100	15:91

(*continued*)

TABLE 1

(Continued)

Marker name	Primers	Repeat class	Allele size (bp) C32, SJD	Map position
fb16f03.x(wz3059.1)	CTCAGCAAAAATTCACAGTTTG/ TGATTGACATGGAGCGAAAA	TA	140, 155	15:97
fd10c06.y(wz13890.1)	TCCATTCAGAGCAGCAAACA/ TTACCTTCTGCTCACTCTTTCAA	CA	145, 175	16:63
fa27g06.s(wz10306.1)	CAAAATGTATGATGTGCATTGTTT/ GAGCCCTGTTTTGAAACTCACTA	AAT	145, 155	17:45
fb79g06.y(wz9729.2)	ACCAGGACGGACGTAAACAC/ CGTCACGATCACATGACACA	GA	100, 90	21:2
fc28c01.x(wz4357.1)	TCGATCGACAGACCAAATCA/ TCGATTGATTGATTGACTGG	AATC	145, 135	21:2
fj61b03.x(wz9739.1)	AGGGACACTTCAGACACTAGAAAG/ TAAAGGGACAAAGCCGAAAA	AATG	125, 95	21:58
fj04d06.x(wz7924.1)	ACAACGTTGGCTTTATGCAC/ GGCGTTGTTGTTATTTTTCCA	ATAG	210, 215	21:89
fb64h06.y(wz3.1)	CACCCGTCTCTTCTGAAAGC/ GAGAGCTGGACAACGAGGAG	GCT	170, 150	22:53
fc92d04.x(wz2481.1)	TGCCTCTGTTCGTTCTCTCA/ TGCAAAGGCTGACATGAAAA	AAT	150, 155	22:100
fj68h04.x(wz16395.1)	CAGTTTAGTTGGCATTGGTGA/ GCAAGCTTCAAAAACAGGAA	ATAG	390, 240	23:42
fi42c02.x(wz9982.1)	GCAGAAATGGTTCATTGAGGA/ TGGCCCAAGAGATAGAGGTC	GA	200, 230	23:51
fa07a07.r(wz9928.1)	CACTGAGTGTATTCTAGGACACTTTT/ TGGCCCAAGAGATAGAGGTC	GA	190, 220	23:57
fi36c02.x(wz5391.2)	ATCCAGTTGCTGCAGGAGTC/ GCTCATCATGCTGACGACAC	CA	170, 80	23:114
fc96f03.x(wz374.1)	GACCATGTTAGGCATTAAAGTTG/ GAGGATTTAGCTGCCTTGTTT	CA	145, 155	23:114
fb93g02.x(wz9367.1)	CGTTCATCTCAGCGTCACTT/ TCAGGGTGAGCTGCTTTGAT	AAAC	85, 90	23:114
fi49c05.x(wz3555.2)	CGTCCGCCTACTTTGTTCAG/ GCGCGGTAAGTGTTTTAAGG	ACGG	100, 90	24:0
fc16b12.x(wz11945.1)	GGCGAAACCGACAAGAGTTA/ TCGGACTGTGAACTGGACAC	AAT	155, 170	24:34
fj98d09.x(wz4488.1)	GGCGGTAATCACATCAAAGG/ GTCCCAGTTTGGGAAGAGGT	AAAC	135, 125	24:56
fj58a12.x(wz2585.1)	GCATTTGGCAAAACTCTCCT/ TGTGAGTATGTGTGTCTGTGAGAG	CA	60, 50	25:0
fj86a09.y(wz16523.1)	GCACAGATTTTTGCACCAGA/ TCTGATGGCGAGACAGACAG	AGAC	140, 95	25:37
fb73a01.x(wz6886.1)	TCCTTCAGGCAATCATGAAA/ TGGAAGGACACAGAGAAATAGGA	GA	135, 145	25:62
fj54a01.x(wz217.1)	TTCTGGTGGAAGACGGAAAC/ TCAAGTGCCACCTCAGTGTC	AAT	140, 160	25:105

Markers are listed by name, with their corresponding EST assembly in parentheses. Also shown are their respective forward/reverse primer sequences, repeat class, allele sizes, and map position (LG:cM; see Meiotic Maps at http://zfish.wustl.edu).

flanking that candidate marker were similarly tested for polymorphism and linkage to refine the mutant map position. After identifying the map position of an individual mutant, corresponding F_2 diploid outcross fish were genotyped to identify individuals carrying the SJD haplotype at the linked markers. These heterozygous carriers were then intercrossed to produce diploid mutants for phenotypic analysis and to confirm the map position. In some cases, map positions were also confirmed by complementation analysis (see below) or half-tetrad analysis. Map positions of mutations identified in this screen and several other embryonic pigment pattern mutants identified in our lab and mapped in this project are shown in Table 3.

In some cases, mutations with similar phenotypes mapped to the same location. For example, alleles *j121e1*,

TABLE 2

SSLP marker panel for first-pass bulked-segregant analysis

Marker	Position (cM)	Allele size (bp) C32, SJD	Marker	Position (cM)	Allele size (bp) C32, SJD
LG1 (99 cM)			LG9 (116 cM)		
z9217	10	180, 150	z10130	2	240, 190
fc27h08	24	120, 290	z5080	43	210, 310
z1154[a]	43	240, 180	z1660[a]	54	250, 240
z24694	70	190, 210	z10789	79	180, 200
z6802	80	190, 210	z7807	89	230, 250
z22347	95	150, 120	z106	116	195, 190
LG2 (119 cM)			LG10 (114 cM)		
z1484	0	190, 180	z9208	2	200, 180
z4469	18	170, 190	z8146	14	200, 180
z4662[a]	46	280, 260	z3835[a]	42	150, 200
z13281	64	150, 180	z11229	72	110, 130
z1406	84	200, 280	z14193	97	180, 160
z7358	103	190, 210	z6754	105	140, 120
LG3 (132 cM)			LG11 (108 cM)		
z3929	3	110, 200	z3527	8	210, 310
z3439	28	120, 140	z8032[a]	30	140, 160
gof14	39	150, 310	z3412	58	180, 150
z22555[a]	77	250, 150	z22038	72	190, 210
z3725	95	260, 290	z13411	88	280, 300
z20058	113	110, 105	z3362	100	190, 210
z1401	129	220, 200	LG12 (112 cM)		
LG4 (111 cM)			z1176	0	240, 270
z20533	10	230, 200	z6920	25	220, 225
z11876	30	180, 185	z1473	37	110, 120
z20450[a]	55	280, 290	z4188[a]	68	210, 220
z984	95	210, 205	z10364	90	200, 180
z25562	111	250, 380	z1312	112	120, 130
LG5 (150 cM)			LG13 (110 cM)		
z3902	11	210, 200	z1531	0	210, 300
z5552	36	220, 200	z9564	20	170, 180
z6614	61	190, 210	z5395	42	210, 180
z13866	78	210, 280	z13250[a]	59	210, 290
z5538[a]	107	210, 310	z26404	81	390, 450
z4299	133	280, 300	z6657	95	130, 190
z34450	145	200, 180	fj03e12	110	120, 100
LG6 (141 cM)			LG14 (118 cM)		
z1265	0	160, 150	z8471	5	300, 200
z9870	32	120, 140	z41025	39	150, 130
z20932[a]	52	210, 300	z11725[a]	55	250, 240
z10183	74	280, 210	z1688	87	300, 290
z1050	100	200, 210	z618	110	180, 200
z19665	121	180, 170	LG15 (110 cM)		
gof20	141	240, 260	z34706	8	200, 250
LG7 (162 cM)			z21982	30	200, 180
z177	2	150, 120	z3358[a]	54	280, 310
z8252	29	220, 200	z9189	68	290, 250
z4999	55	260, 290	z13822	84	160, 150
z10487	83	130, 110	z5223	110	180, 210
z8604[a]	98	280, 250	LG16 (129 cM)		
z1535	141	180, 160	z1642	0	210, 230
fj30f10	162	110, 190	z21155	24	140, 110
LG8 (112 cM)			z3104[a]	54	250, 300
z9420	12	320, 150	z19632	85	190, 220
z987	29	200, 280	z4670	98	190, 150
fi59h04[a]	57	180, 160	z15453	116	205, 195
fk30a11	75	140, 180			

(*continued*)

TABLE 2

(Continued)

Marker	Position (cM)	Allele size (bp) C32, SJD	Marker	Position (cM)	Allele size C32, SJD
LG17 (104 cM)			LG21 (110 cM)		
z652	0	120, 130	z14506	8	180, 200
z1490	10	205, 200	z7423	22	290, 340
z22674	33	180, 200	z21106[a]	52	290, 310
z15715	57	140, 110	z4425[a]	72	180, 150
z1408[a]	69	220, 400	z42626	95	290, 210
z4053	78	200, 210	z11113	110	190, 240
z3123	104	140, 160	LG22 (100 cM)		
LG18 (124 cM)			z11752	0	150, 180
z5231	12	120, 110	z10673	20	280, 210
z13329	21	140, 120	z13223[a]	46	210, 180
z8488	45	120, 200	z11679	57	190, 200
z737[a]	71	180, 170	z28677	100	290, 310
z9941	101	280, 310	LG23 (115 cM)		
z1417	124	140, 130	z11407	0	260, 210
LG19 (98 cM)			z4003	22	230, 220
z1625	3	220, 150	z20039[a]	42	180, 170
z3782	24	120, 190	z4421	68	200, 220
z3816[a]	52	200, 170	z3525	94	160, 180
z22532	65	230, 320	z3157	100	140, 110
z6661	92	150, 140	fc96f03	114	120, 150
LG20 (113 cM)			LG24 (84 cM)		
z9334	6	130, 150	z1584	6	180, 190
z3824[a]	44	210, 270	z9852[a]	29	280, 260
z10756	55	200, 230	z249	59	150, 140
z9794	76	210, 180	z9325	74	210, 250
z7171	100	300, 220	LG25 (108 cM)		
z374	113	180, 200	z11092	0	180, 140
			gof1	19	180, 210
			z20832	39	210, 290
			z8224[a]	54	230, 260
			z3528	81	190, 240
			z1431	108	180, 210

Panel markers are listed by linkage group (LG), with corresponding map position and allele sizes shown in adjacent columns. The total length of each LG is shown in parentheses next to its respective heading.

[a] The suggested centromere marker for each linkage group (Johnson *et al.* 1996).

j121e2, *j121e3*, and *j121e4* all mapped near gof1 on LG25 and failed to complement each other when carriers were interbred. Similarly, alleles *j126e1* and *j126e2* mapped near z4421 on LG23 and failed to complement each other. Because these alleles may have been derived from the same mutagenized male, it is not yet clear whether these are indeed independent alleles or multiple isolates of the same allele (except for *j121e1*, which was derived from a different mutagenized male than *j121e2–4*). In other instances, new mutants mapped to the same locations as previously identified pigment pattern loci, directing us to test for allelism by complementation analysis. For example, allele *j1e249* mapped to z10756 on LG20, the map position of the *kit* receptor tyrosine kinase gene (also called *sparse*; Parichy *et al.* 1999). We found that *j1e249* mutants failed to complement the *kit*^{b5} null allele when carriers were interbred, confirming that *j1e249* is an allele of *kit*. Similarly, allele *j124e1* was mapped to near z11685 and z7654 on LG18, the recently identified map position of *touchtone* (B. Arduini and P. Henion, personal communication). Interbreeding of *j124e1* and *touchtone*^{as1} carriers showed a failure to complement, demonstrating that *j124e1* is an allele of *touchtone*. Finally, *j125e1* mapped to z4999 on LG7, near the recently identified map position of *endzone* (B. Arduini and P. Henion, personal communication). In contrast to *kit* and *touchtone*, interbreeding of *endzone*^{b431} (Henion *et al.* 1996) and *j125e1* carriers revealed complementation, indicating that *j125e1* and *endzone* are different genes.

Melanocyte mutant phenotypes: Zebrafish melanocytes first become visible beginning around 1 dpf, as expression of melanin pigment begins in the PRE and in neural-crest-derived melanocytes (Kimmel *et al.* 1995). Some neural-crest-derived melanocytes remain at the dorsal aspect of the neural tube, while others migrate

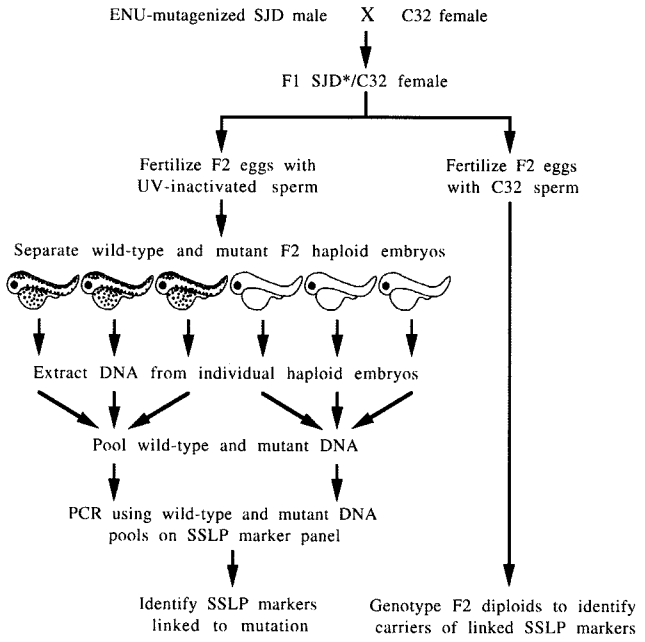

FIGURE 1.—Design of F_2 haploid screen for melanocyte mutants and subsequent bulked-segregant mapping.

to positions throughout the body to comprise the embryonic melanocyte pattern (Figure 2, A and B). This pattern largely persists through the larval stages (MILOS and DINGLE 1978) until the onset of larval-adult metamorphosis beginning ~14 dpf (JOHNSON *et al.* 1995b). The embryonic melanocyte mutants identified and mapped in this work are defective for distinct aspects of melanocyte development, allowing them to be grouped into several phenotypic classes. These phenotypic classes are discussed below, with reference to previously identified zebrafish melanocyte mutants. As most of the previously identified melanocyte mutations remain unmapped, it is unclear whether they are candidate alleles of the new mutations reported here (see DISCUSSION). In naming these new melanocyte mutant loci, we have followed our custom of naming lethal melanocyte mutations after deceased or extinct cats and viable melanocyte mutations after extant cats.

Mutations causing degeneration of all melanocytes: Mutations at *perruque* (Figure 2, C and D) and *blatherskite* (not shown) cause degeneration of both neural-crest-derived and PRE melanocytes. In these phenotypes, neural-crest-derived melanocytes initially appear smaller than wild type but in a relatively normal distribution, while the PRE initially appears pale (Figure 2C). Both types of melanocytes then degenerate and disappear over subsequent days of development (Figure 2D). The *blatherskite*^{j122e1} allele also shows brain degeneration beginning ~3 dpf (not shown). Together, these defects resemble those observed in the previously identified mutants *delayed fade*, *fade out*, *fading vision*, *blurred*, *ivory* (KELSH *et al.* 1996), *piegus*, *punktata*, and *mizerny* (MALICKI *et al.* 1996).

TABLE 3

Melanocyte mutation map positions

Locus name	Allele name	LG	Marker	Linkage[f]
serpolet (*srp*)	*j123e1*	5	z4299	15/18[g]
pinky (*pnk*)	*j125e1*[a]	7	z4999	22/23[g]
selima (*sel*)	*j108e1*	7	z1239[e]	22/22[g]
		7	z1535	21/21[g]
cheshire (*chs*)	*j129e1*	9	z5394[e]	23/24[g]
		9	z9754[e]	22/24[g]
rubis (*rub*)	*j127e1*	17	z15715	20/23
touchtone (*tct*)	*j124e1*	18	z11685[e]	19/19[g]
		18	z7654[e]	19/19[g]
kit (*kit*)	*j1e249*	20	z10756	20/20[g]
sourmash (*srm*)	*j117e1*[b]	21	z7423[e]	20/20
		21	z15891[e]	20/21
	j118e1[b,c]	21	z7423[e]	18/18[g]
		21	z15891[e]	18/18[g]
	j130e1[b,c]	21	z7423[e]	22/22[g]
		21	z15891[e]	19/19[g]
racan (*rcn*)	*j128e1*	21	z7423	19/19[g]
tammany (*tam*)	*j120e1*	22	z10673	15/17
blatherskite (*bsk*)	*j122e1*	22	z13223	19/20[g]
perruque (*prq*)	*j126e1*[b]	23	z20039	23/25[g]
		23	z4421	23/25[g]
	j126e2[b]	23	z20039	19/24[g]
		23	z4421	22/23[g]
chloe (*chl*)	*j121e1*[d]	25	gof1	21/21[g]
	j121e2[d]	25	gof1	15/16[g]
	j121e3[d]	25	gof1	18/20[g]
	j121e4[d]	25	gof1	19/20[g]

[a] Complementation tests between *j125e1* and *endzone*^{b431} suggest that they are different genes.

[b] These isolates may have been derived from the same mutagenized male and therefore might represent only one allele.

[c] Provisional locus assignments (complementation analysis not performed).

[d] The *j121e1* allele was derived from a different mutagenized male than *j121e2–4*; therefore these four isolates represent at least two different alleles.

[e] Markers not included in Table 2 that also display robust polymorphism between C32 and SJD.

[f] Cosegregation of mutant phenotype with SJD allele at marker at left in haploids.

[g] Linkage confirmed by independent tests (including half-tetrad analysis, complementation analysis, or progeny testing).

Mutations causing deficiencies in PRE melanocytes: Mutant alleles of *sourmash* (Figure 2, E and F) are deficient for PRE melanocytes, but develop a normal pattern of neural-crest-derived melanocytes. This mutant phenotype resembles the previously identified retina mutants *oko meduzy*, *glass onion*, *nagie oko*, and *heart and soul* (MALICKI *et al.* 1996).

Mutations causing defects in melanin synthesis: Mutations at *rubis*, *chloe*, and *racan* cause deficiencies in melanin synthesis. The *rubis*^{j127e1} allele results in the complete absence of melanin in both neural-crest-derived and PRE melanocytes (not shown). Mutations in *chloe* (Fig-

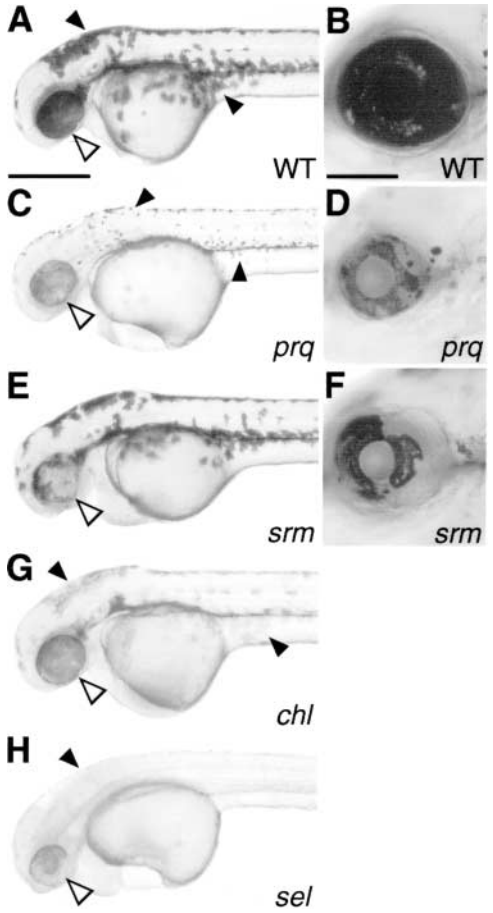

FIGURE 2.—Mutations affect distinct aspects of embryonic melanocyte development. Wild-type (WT) embryos at 2 dpf (A) have darkly pigmented neural-crest-derived melanocytes along the dorsal stripe and over the yolk (solid arrowheads). The PRE is also darkly pigmented by 2 dpf (open arrowhead) and continues to develop to contribute to the functional eye organ by 5 dpf (B). Mutations at *perruque*^{j126e1} (*prq*) cause punctate neural-crest-derived melanocytes at 2 dpf (C, solid arrowheads), while the PRE remains faint (open arrowhead) and begins to degenerate by 5 dpf (D). In *sourmash*^{j118e1} (*srm*) mutants, the PRE is largely absent at 2 dpf (E, open arrowhead) and does not recover through 5 dpf (F). *chloe*^{j121e1} (*chl*, G) mutants have normal distribution and morphology of neural-crest-derived (solid arrowheads) and PRE melanocytes (open arrowhead), yet they fail to become fully pigmented. The *selima*^{j108e1} (*sel*, H) mutation causes a severe deficit of neural-crest-derived melanocytes (solid arrowhead) and defective PRE development (open arrowhead). All mutants shown are homozygous. Bars, 400 μm (A, C, E, G, and H) and 200 μm (B, D, and F).

ure 2G) and *racan* (not shown) result in substantially delayed and incomplete melanization in both neural-crest-derived and PRE melanocytes. However, the individual morphology of embryonic melanocytes and their resulting pattern are largely normal in these two mutant phenotypes, suggesting that these animals are deficient for melanin synthesis. Since *chloe*, *racan*, and *rubis* map to different linkage groups, they represent distinct loci. The embryonic phenotypes of *chloe*, *racan*, and *rubis* are similar to those caused by previously isolated mutations at *albino* (CHAKRABARTI *et al.* 1983), *golden*, *brass* (STREISINGER *et al.* 1986), *casper* (HENION *et al.* 1996), *lead*, *mustard*, *nickel*, *pewter*, *sandy*, and *brassy* (KELSH *et al.* 1996). Interestingly, all alleles of *chloe* isolated in this study are viable and result in adults displaying severe melanocyte and iridophore deficiencies.

Mutations causing reduction of neural-crest-derived melanocytes: Mutations at *pinky* cause a substantial reduction in the number of neural-crest-derived melanocytes, in addition to severe anterior-posterior body axis defects (not shown). We identified one mutant, *selima*, that lacked virtually all neural-crest-derived melanocytes. Homozygous *selima* mutants develop pale PRE and display a number of other pleiotropic defects after 2 dpf (Figure 2H). These melanocyte deficiency phenotypes resemble those of previously identified mutations at *endzone* (HENION *et al.* 1996), *colorless*, *white tail* (KELSH *et al.* 1996), *nacre* (LISTER *et al.* 1999), and *alyron* (CRETEKOS and GRUNWALD 1999).

Mutations affecting melanocyte morphology: Neural-crest-derived melanocytes in wild-type embryos usually appear stellate with uniform pigmentation (Figure 3, A and B). We identified two mutants, *cheshire*^{j129e1} (Figure 3, C and D) and *touchtone*^{j124e1} (not shown), that develop melanocytes with varying morphologies and pigmentation. In these phenotypes, neural-crest-derived melanocytes appear either pale with normal stellate morphology or punctate with apparently normal melanization. Through the first week of development, some of the punctate melanocytes appear to be extruded through the epidermis. These phenotypes resemble those seen in previously identified mutant alleles at *touchtone* (B. ARDUINI and P. HENION, unpublished results), *cold-light*, *polished*, *freckles*, and *punkt* (KELSH *et al.* 1996). As mentioned above, allele *j124e1* was identified as an allele of *touchtone* first by our mapping efforts and subsequently by complementation testing.

Mutations affecting melanocyte migration: We identified three mutant alleles, *serpolet*^{j123e1} (not shown), *tammany*^{j120e1} (not shown), and *kit*^{j1e249} (Figure 4), which were defective for melanocyte migration. In these phenotypes, neural-crest-derived melanocytes largely failed to migrate properly away from the dorsal aspect of the neural tube. The *kit*^{j1e249} allele was found to be temperature sensitive, with homozygotes reared at 25° developing a wild-type melanocyte pattern (Figure 4, A and B) and those reared at 33° displaying melanocyte migration defects at 2.5 dpf (Figure 4C). In contrast to the *kit* null allele phenotype, where neural-crest-derived melanocytes begin to die by 4 dpf and are largely absent by 7.5 dpf (see PARICHY *et al.* 1999), melanocytes in *kit*^{j1e249} homozygotes reared at 33° persist through 7.5 dpf (Figure 4D). These melanocyte migration phenotypes resemble those of previously isolated mutant alleles at *kit* (PARICHY *et al.* 1999) and *sparse-like* (KELSH *et al.* 1996).

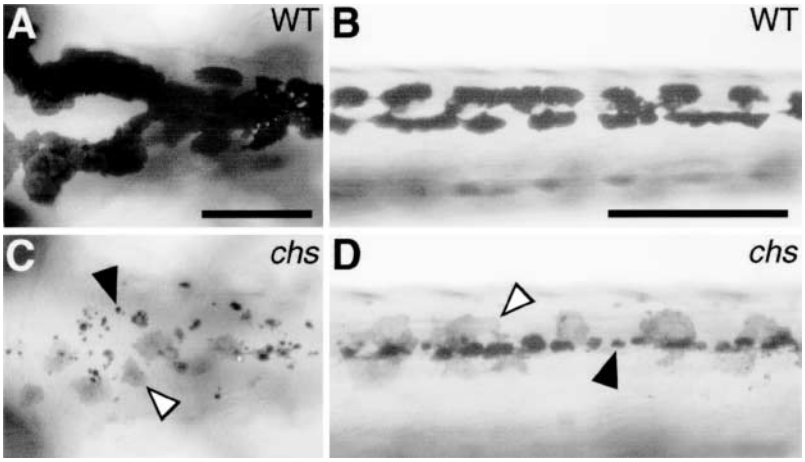

FIGURE 3.—Mutation at *cheshire* causes variable melanocyte morphologies. Wild-type (WT) neural-crest-derived melanocytes on the dorsal aspect of the head at 2.5 dpf (A) and in the dorsal stripe at 6 dpf (B) are all stellate and darkly pigmented. Homozygous *cheshire*^{j129e1} (*chs*) mutants at 2.5 dpf (C) and 6 dpf (D) show both punctate darkly pigmented melanocytes (solid arrowheads) and faintly pigmented stellate melanocytes (open arrowheads) within the dorsal stripe. Bars, 200 μm.

DISCUSSION

Powerful forward genetics is one of the principal advantages of the zebrafish model system. However, managing mutant lines, mapping mutations, and positionally cloning the affected genes remain laborious tasks. Therefore, an important challenge facing zebrafish workers is to develop techniques to simplify and to accelerate these processes. Among the approaches that might help meet these challenges are the development of highly polymorphic inbred lines, the derivation of those polymorphisms into reliable markers, and the exploitation of those polymorphic markers to expedite and enhance the mapping process. Here we have taken advantage of the polymorphism between the C32 and SJD inbred lines by developing a minimal first-pass panel of SSLP markers for these strains and then using that panel in bulked-segregant analysis to rapidly map a set of new melanocyte mutants.

The ability to distinguish between alleles from different strains is essential to all common mutant mapping approaches in zebrafish. DNA sequence polymorphisms present between mapping strains and the markers derived from them generally provide this ability. For example, bulked-segregant analysis depends on the ability to assess linkage of mutations to polymorphic markers located along each linkage group (MICHELMORE *et al.* 1991). Our work identifies a minimal panel of SSLP markers between SJD and C32 that can be used in bulked-segregant analysis to rapidly identify map positions of new mutations. Importantly, the mapping approach described here is relatively simple and inexpensive, allowing it to be performed even in small laboratories with modest budgets.

The intention of this work was to develop a rapid and reliable technique for determining the map position of new zebrafish mutations as they are identified in mutagenesis screens. By coupling mutagenesis screens to mapping of the resulting mutants, we hoped to facilitate several subsequent tasks. First, the rapid mapping of new mutations simplifies the task of stock management. By identifying SSLP markers closely linked to a mutant locus, recognition of heterozygous carriers can be accomplished through PCR-based genotyping, instead of through more laborious progeny testing. In our study, this method of carrier identification allowed us to quickly identify F_2 outcross siblings heterozygous at markers linked to the respective mutation.

Second, the rapid mapping of new mutations helps to direct allelism testing against previously identified mutant loci. Previous mutagenesis screens in zebrafish have produced thousands of mutant lines, many with similar phenotypes. After isolating new mutations, ze-

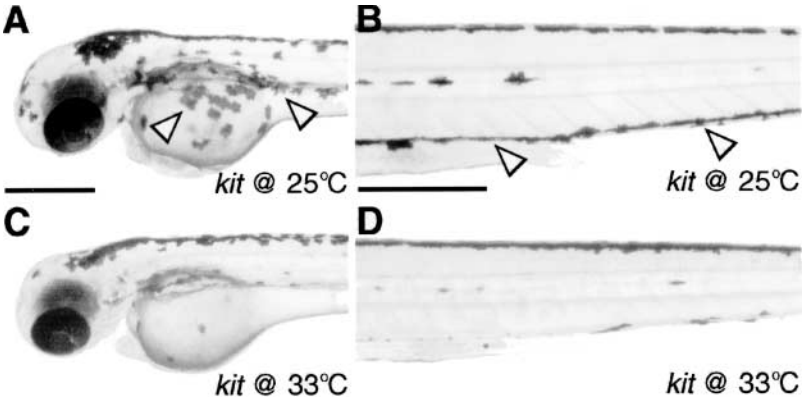

FIGURE 4.—Temperature-sensitive mutation at *kit* affects melanocyte migration. When reared at 25°, neural-crest-derived melanocytes in *kit*^{j1e249} (*kit*) mutants migrate normally into ventral positions by 2.5 dpf (A, open arrowheads) and persist in these ventral locations through 7.5 dpf (B, open arrowheads). In contrast, neural-crest-derived melanocytes in *kit*^{j1e249} mutants reared at 33° fail to migrate to these ventral positions by 2.5 dpf (C), yet persist through 7.5 dpf (D). All mutants shown are homozygous. Bars, 200 μm.

brafish workers are then challenged to distinguish between new mutations at previously identified loci and mutations at novel loci. Since these mutant lines are often maintained in separate laboratories, often on different continents, complementation testing of all possible permutations is a nontrivial task. Identification of map locations first can be used to unambiguously exclude the possibility of allelism for many mutations (see below). Because initial mapping in zebrafish has become relatively inexpensive (especially compared to costs of exchanging stocks between labs), this provides a useful alternative to the complementation test in the management of mutant screens. In those instances in which mutations with similar phenotypes do map to the same genomic region, the complementation test is then compelled to determine whether the mutations affect the same gene. Because few mutations in zebrafish are mapped, the identification of map positions for mutations identified here will provide candidate positions for those pigmentation mutations with similar phenotypes that remain unmapped. We also imagine that coupled mutagenesis and mapping, as described here, can be used in new mutagenesis screens to rapidly select for mutations at previously uncharacterized loci.

To demonstrate the efficacy of this approach, we subjected the new mutations described here to the analysis discussed above. After initial mapping, we found that several mutations mapped to the same genomic regions as known pigment pattern loci. We then performed complementation analyses to test for allelism. These tests revealed that *j124e1* is a new allele of *touchtone* and that *j1e249* is a new allele of *kit*. Complementation in crosses between carriers for *pinky*^{j125e1} and *endzone*, which map to a similar region on LG7, tends to exclude allelism of these mutations. Similarly, identification of mutations with similar map positions within this screen compelled complementation tests that revealed that *j121e1*, *j121e2*, *j121e3*, and *j121e4* are all alleles of the *chloe* locus and that *j126e1* and *j126e2* are both alleles of the *perruque* locus. (Note that we assign allele names after mapping and complementation tests are completed; see MATERIALS AND METHODS.)

By comparing the map positions of new mutations to previously identified mutations with similar phenotypes, we were also able to exclude a substantial fraction of these known mutations as potentially allelic to the new mutations described here. These results are discussed below.

We identified several mutations that affect melanin synthesis, including *rubis* (LG17), *chloe* (LG25), and *racan* (LG21 at 22 cM). While several melanin synthesis mutations have been previously reported, the majority of these can be excluded as possibly allelic to our new mutations on the basis of their map positions. Specifically, the melanin synthesis mutations *albino* (LG21 at 52cM), *brass* (LG13; POSTLETHWAIT *et al.* 1994), *golden* (LG18; see http://zfin.org), and *sandy* (LG15; W. STAUB and H. BAIER, personal communication) do not map to the same genomic regions as the new mutations described here, while the map positions of *casper* (HENION *et al.* 1996), *lead*, *mustard*, *nickel*, *pewter*, and *brassy* (KELSH *et al.* 1996) remain unknown. The map positions of *rubis*, *chloe*, and *racan* therefore provide candidate positions for the remaining unmapped melanin synthesis mutations listed above or for additional melanin synthesis mutations isolated in the future.

Mutations at *sourmash* (LG21) were found to cause PRE defects similar to several previously described mutations. That PRE mutations *nagie oko* and *heart and soul* map to different linkage groups (LG17 and LG2, respectively; HORNE-BADOVINAC *et al.* 2001; WEI and MALICKI 2002) excludes the possibility that *sourmash* is an allele of either of those genes. It remains possible that other, yet unmapped, PRE mutations, such as *glass onion* or *oko meduzy* (MALICKI *et al.* 1996), correspond to *sourmash*.

In addition to the new *kit* allele (*j1e249*) identified in this screen (see above), we identified and mapped mutations at two additional loci that affected migration of neural-crest-derived melanocytes: *serpolet* (LG5) and *tammany* (LG22). Since only one other melanocyte migration mutation has been identified (*sparse-like*; KELSH *et al.* 1996), our map positions for *serpolet* and *tammany* provide two candidate map locations for *sparse-like* and identify at least one novel locus required for melanocyte migration.

Two mutations identified in this screen, *pinky* (LG7 at 55 cM) and *selima* (LG7 at 125–141 cM), caused reduction in the number of neural-crest-derived melanocytes. Several mutations that cause reduction in neural-crest-derived melanocytes have been identified and mapped, including *colorless* (LG3; DUTTON *et al.* 2001), *nacre* (LG6; LISTER *et al.* 1999), *alyron* (LG15; CRETEKOS and GRUNWALD 1999), and *endzone* (LG7 at ~55 cM; B. ARDUINI and P. HENION, personal communication; see above for discussion of nonallelism between *endzone* and *pinky*). Therefore, *selima* and *pinky* provide candidate positions for the remaining unmapped mutation described in this class, *white tail* (KELSH *et al.* 1996).

In addition to the new *touchtone* (LG18) allele (*j124e1*) identified in this screen, we identified a mutation at one other locus, *cheshire* (LG9), that results in mixed melanocyte morphologies. This is similar to mutations at *cold light*, *polished*, *freckles*, and *punkt* (KELSH *et al.* 1996). Since map positions for these mutations have not been reported, it remains unclear whether *cheshire* identifies a novel locus or instead provides a candidate map position for these genes.

We also identified and mapped mutations at two loci, *blatherskite* (LG22) and *perruque* (LG23), that cause melanocyte degeneration phenotypes similar to previously identified mutations at *delayed fade*, *fade out*, *fading vision*, *blurred*, *ivory* (KELSH *et al.* 1996), *piegus*, *punktata*, and *mizerny* (MALICKI *et al.* 1996). Since map positions have not been reported for these mutations, it remains un-

clear whether *blatherskite* and *perruque* identify new loci or may provide candidate positions for previously identified members of this class.

Finally, the rapid initial mapping of new mutations will accelerate the identification of candidate genes. With the availability of dense gene maps (Geisler *et al.* 1999; Barbazuk *et al.* 2000) and the imminent completion of the zebrafish genome, the map position of a new mutation could quickly yield a list of relevant candidate genes in the genomic region. This technique could also be used to screen for mutations linked to specific candidate genes of interest.

Although our efforts described here should help accelerate the initial mapping of mutations, improvements are still needed in this and subsequent steps. For example, increasing the density of reliable SSLPs and SNPs between C32 and SJD should accelerate further resolution of the mutant map positions suggested by initial mapping efforts. A potential problem in mapping may arise from our reciprocal introgression schemes to remediate sex ratios in SJD or lack of vigor in C32 inbred strains (see materials and methods). This scheme may result in residual blocks of introgressed donor DNA in the host chromosomes unrelated to the selected trait. Thus, in crosses between the new C32 and SJD lines, there may be some regions that are not informative. The number and extent of these regions will likely be quite small, as the effect of sequential backcrosses is to serially dilute out the unselected donor DNA. If there is no effect of selection on the maintenance of donor DNA, we would expect the level of donor contamination summed between these two lines to be $<1\%$ ($<0.2\%$ SJD DNA in the invigorated C32 strain following nine sequential backcrosses and $<0.4\%$ donor C32 DNA in the feminized SJD lines following eight sequential backcrosses). In practice, the effect of selection for vigor or for enhanced sex ratios may be to retain more heterozygosity, resulting in a somewhat higher amount of donor DNA in the introgression lines. Such heterozygosity can be detected by PCR-based screens, using the first-pass panel described here, or ultimately, by resequencing the genomes of each strain (for instance, see Mitra and Church 1999). The problem of residual donor DNA may also be remediated by using crosses to a third strain, such as WIK, in subsequent mapping experiments. WIK, albeit not inbred, is highly polymorphic with both C32 and SJD (Nechiporok *et al.* 1999).

We expect that the success of this approach with respect to SJD and C32 inbred lines will prompt development of additional inbred lines. Additional first-pass marker panels specific to different pairs of genetic backgrounds may also extend the usefulness of this approach, further facilitating the rapid mapping of mutations and management of mutagenesis screens. Importantly, such reagents will be useful in managing not only haploid screens as described here, but also early pressure parthenogenesis screens (Johnson and Weston 1995; Henion *et al.* 1996) or F_3 intercross screens (Driever *et al.* 1996; Haffter *et al.* 1996a).

The authors thank Colleen Boggs, Sarah Callier, and Steven Jacobs for fish husbandry. The authors are especially grateful to Wendy Straub and Herwig Baier for sharing unpublished map data, and to Brigitte Arduini and Paul Henion for sharing unpublished map data and performing complementation tests. This work was supported by National Institutes of Health grant R01-GM56988.

LITERATURE CITED

Barbazuk, W. B., I. Korf, C. Kadavi, J. Heyen, S. Tate *et al.*, 2000 The syntenic relationship of the zebrafish and human genomes. Genome Res. **10:** 1351–1358.

Chakrabarti, S., G. Streisinger, F. Singer and C. Walker, 1983 Frequency of gamma-ray induced specific locus and recessive lethal mutations in mature germ cells of the zebrafish, *Brachydanio rerio.* Genetics **103:** 109–124.

Clark, M. D., S. Hennig, R. Herwig, S. W. Clifton, M. A. Marra *et al.*, 2001 An oligonucleotide fingerprint normalized and expressed sequence tag characterized zebrafish cDNA library. Genome Res. **11:** 1594–1602.

Cretekos, C. J., and D. J. Grunwald, 1999 *alyron*, an insertional mutation affecting early neural crest development in zebrafish. Dev. Biol. **210:** 322–338.

Driever, W., L. Solnica-Krezel, A. F. Schier, S. C. F. Neuhauss, J. Malicki *et al.*, 1996 A genetic screen for mutation affecting embryogenesis in zebrafish. Development **123:** 37–46.

Dutton, K. A., A. Pauliny, S. S. Lopes, S. Elworthy, T. J. Carney *et al.*, 2001 Zebrafish *colourless* encodes *sox10* and specifies non-ectomesenchymal neural crest fates. Development **128:** 4113–4125.

Farber, S. A., M. Pack, S.-Y. Ho, I. D. Johnson, D. S. Wagner *et al.*, 2001 Genetic analysis of digestive physiology using fluorescent phospholipid reporters. Science **292:** 1385–1388.

Geisler, R., G. J. Rauch, H. Baier, F. Van Bebber, L. Brobeta *et al.*, 1999 A radiation hybrid map of the zebrafish genome. Nat. Genet. **23:** 86–89.

Haffter, P., M. Granato, M. Brand, M. C. Mullins, M. Hammerschmidt *et al.*, 1996a The identification of genes with unique and essential functions in the development of the zebrafish, *Danio rerio.* Development **123:** 1–36.

Haffter, P., J. Odenthal, M. C. Mullins, S. Lin, M. J. Farrell *et al.*, 1996b Mutations affecting pigmentation and shape of the adult zebrafish. Dev. Genes Evol. **206:** 260–276.

Henion, P. D., D. W. Raible, C. E. Beattie, K. L. Stoesser, J. A. Weston *et al.*, 1996 Screen for mutations affecting development of zebrafish neural crest. Dev. Genet. **18:** 11–17.

Herron, B. J., W. Lu, C. Rao, S. Liu, H. Peters *et al.*, 2002 Efficient generation and mapping of recessive developmental mutations using ENU mutagenesis. Nat. Genet. **30:** 185–189.

Horne-Badovinac, S., D. Lin, S. Waldron, M. Schwarz, G. Mbamalu *et al.*, 2001 Positional cloning of *heart and soul* reveals multiple roles for PKC lambda in zebrafish organogenesis. Curr. Biol. **11:** 1492–1502.

Hukriede, N. A., L. Joly, M. Tsang, J. Miles, P. Tellis *et al.*, 1999 Radiation hybrid mapping of the zebrafish genome. Proc. Natl. Acad. Sci. USA **96:** 9745–9750.

Hukriede, N., D. Fisher, J. Epstein, L. Joly, P. Tellis *et al.*, 2001 The LN54 radiation hybrid map of zebrafish expressed sequences. Genome Res. **11:** 2127–2132.

Jagadeeswaran, P., M. Gregory, S. Johnson and B. Thankavel, 2000 Haemostatic screening and identification of zebrafish mutants with coagulation pathway defects: an approach to identifying novel haemostatic genes in man. Brit. J. Haematol. **110:** 946–956.

Johnson, S. L., and J. A. Weston, 1995 Temperature-sensitive mutations that cause stage-specific defects in zebrafish fin regeneration. Genetics **141:** 1583–1595.

Johnson, S. L., D. Africa, S. Horne and J. H. Postlethwait, 1995a Half-tetrad analysis in zebrafish: mapping the *ros* mutation and the centromere of linkage group I. Genetics **139:** 1727–1735.

Johnson, S. L., D. Africa, C. Walker and J. A. Weston, 1995b Gen-

etic control of adult pigment stripe development in zebrafish. Dev. Biol. **167:** 27–33.

Johnson, S. L., M. A. Gates, M. Johnson, W. S. Talbot, S. Horne *et al.*, 1996 Centromere-linkage analysis and consolidation of the zebrafish genetic map. Genetics **142:** 1277–1288.

Kasarskis, A., K. Manova and K. V. Anderson, 1998 A phenotype-based screen for embryonic lethal mutations in the mouse. Proc. Natl. Acad. Sci. USA **95:** 7485–7490.

Kelly, P. D., F. Chu, I. G. Woods, P. Ngo-Hazelett, T. Cardozo *et al.*, 2000 Genetic linkage mapping of zebrafish genes and ESTs. Genome Res. **10:** 558–567.

Kelsh, R. N., M. Brand, Y.-J. Jiang, C.-P. Heisenberg, S. Lin *et al.*, 1996 Zebrafish pigmentation mutations and the processes of neural crest development. Development **123:** 369–389.

Kimmel, C. B., W. W. Ballard, S. R. Kimmel, B. Ullmann and T. F. Schilling, 1995 Stages of embryonic development of the zebrafish. Dev. Dyn. **203:** 253–310.

Lister, J. A., C. P. Robertson, T. Lepage, S. L. Johnson and D. W. Raible, 1999 *nacre* encodes a zebrafish microphthalmia-related protein that regulates neural-crest-derived pigment cell fate. Development **126:** 3757–3767.

Malicki, J., S. C. F. Neuhauss, A. F. Schier, L. Solnica-Krezel, D. L. Stemple *et al.*, 1996 Mutations affecting development of the zebrafish retina. Development **123:** 263–273.

Michelmore, R. W., I. Paran and R. V. Kesseli, 1991 Identification of markers linked to disease-resistance genes by bulked segregant analysis: a rapid method to detect markers in specific genomic regions by using segregating populations. Proc. Natl. Acad. Sci. USA **88:** 9828–9832.

Milos, N., and A. D. Dingle, 1978 Dynamics of pigment pattern formation in the zebrafish, *Brachydanio rerio*. I. Establishment and regulation of the lateral line melanophore stripe during the first eight days of development. J. Exp. Zool. **205:** 205–216.

Mitra, R. D., and G. M. Church, 1999 *In situ* localized amplification and contact replication of many individual DNA molecules. Nucleic Acids Res. **27:** e34.

Nechiporuk, A., J. E. Finney, M. T. Keating and S. L. Johnson, 1999 Assessment of polymorphism in zebrafish mapping strains. Genome Res. **9:** 1231–1238.

Odenthal, J., K. Rossnagel, P. Haffter, R. N. Kelsh, E. Vogelsang *et al.*, 1996 Mutations affecting xanthophore pigmentation in the zebrafish, *Danio rerio*. Development **123:** 391–398.

Parichy, D. M., J. F. Rawls, S. J. Pratt, T. T. Whitfield and S. L. Johnson, 1999 Zebrafish *sparse* corresponds to an orthologue of c-*kit* and is required for the morphogenesis of a subpopulation of melanocytes, but is not essential for hematopoiesis or primordial germ cell development. Development **126:** 3425–3436.

Patton, E. E., and L. I. Zon, 2001 The art and design of genetic screens: zebrafish. Nat. Rev. Genet. **2:** 956–966.

Postlethwait, J. H., S. L. Johnson, C. N. Midson, W. S. Talbot, M. Gates *et al.*, 1994 A genetic linkage map for the zebrafish. Science **264:** 699–703.

Rawls, J. F., and S. L. Johnson, 2001 Requirements for the *kit* receptor tyrosine kinase during regeneration of zebrafish fin melanocytes. Development **128:** 1943–1949.

Rawls, J. F., E. M. Mellgren and S. L. Johnson, 2001 How the zebrafish gets its stripes. Dev. Biol. **240:** 301–314.

Shimoda, N., E. W. Knapik, J. Ziniti, C. Sim, E. Yamada *et al.*, 1999 Zebrafish genetic map with 2000 microsatellite markers. Genomics **58:** 219–232.

Singer, A., H. Perlman, Y. Yan, C. Walker, G. Corley-Smith *et al.*, 2002 Sex-specific recombination rates in zebrafish (*Danio rerio*). Genetics **160:** 649–657.

Solnica-Krezel, L., A. F. Schier and W. Driever, 1994 Efficient recovery of ENU-induced mutations from the zebrafish germline. Genetics **136:** 1401–1420.

Streisinger, G., C. Walker, N. Dower, D. Knauber and F. Singer, 1981 Production of clones of homozygous diploid zebra fish (*Brachydanio rerio*). Nature **291:** 293–296.

Streisinger, G., F. Singer, C. Walker, D. Knauber and N. Dower, 1986 Segregation analysis and gene-centromere distances in zebrafish. Genetics **112:** 311–319.

Walker, C., 1999 Haploid screens and gamma-ray mutagenesis. Methods Cell Biol. **60:** 43–70.

Wei, X., and J. Malicki, 2002 *nagie oko*, encoding a MAGUK-family protein, is essential for cellular patterning of the retina. Nat. Genet. **31:** 150–157.

Communicating editor: D. J. Grunwald